Vietnam Journal of Science and Technology ***59*** *(3) (2021) 357-367*
doi:10.15625/2525-2518/59/3/14703

ON MODELS WITH WOBBLING DISK FOR BRAKE SQUEAL

Nguyen Thai Minh Tuan[1, *], Nils Gräbner[2]

[1]*Hanoi University of Science and Technology, 1 Dai Co Viet, Hai Ba Trung, Ha Noi, Viet Nam*

[2]*Chair of Mechatronics and Machine Dynamics, Technische Universität Berlin, 10587 Berlin*

[*]Email: *tuan.nguyenthaiminh@hust.edu.vn*

Received: 17 December 2019; Accepted for publication: 3 March 2021

Abstract. Among many mathematical models of disk brakes for the explanation of brake squeal, models with wobbling disk have their own advantage over planar models. In planar models, the macroscopic angular velocity of the disk does not appear in the equations of motion, which is contrary to experiments, in which brake squeal only occurs in a certain speed range. In contrast, with the consideration of the spatial motion of the disk, the models with wobbling disk can be used to analyze the influence of the macroscopic angular velocity on the stability behavior. Previous studies have used a specialized commercial software to establish the equations of motion of those models. Applying a recently developed matrix form of Euler equations in rigid body dynamics, the equations establishment process can now be performed with almost all popular computing softwares. Furthermore, the presented models are more generalized in terms of damping, in-plane vibration, and asymmetry. The equations of motion for a 2DOF case that are compact enough are presented. It is shown that asymmetric coefficients of kinetic friction may have stabilizing effect while softening the tangential pads' supports can either stabilize or destabilize the trivial solution of the system.

Keywords: Matrix Form of Euler Equations, Brake Squeal, Wobbling Disk.

Classification numbers: 5.4.1, 5.4.2.

1. INTRODUCTION

There are a lot of low-DOF planar models for the explanation of brake squeal – which is considered to occur when the "silent motion" is unstable. Several studies have related the instability to the negative slope of friction coefficient versus relative velocity [1] while some others have shown that adding springs and/or flexible bodies into a brake system model in an appropriate way can also produce instability due to the skew counterpart of the stiffness matrix [2, 3], but all of them cannot explain the dependence of stability behavior on the macroscopic angular velocity of the disk, which is observed in experiments. Unlike the above-mentioned models, a real disk may deform in a three-dimensional manner, leading to the appearance of gyroscopic terms and a friction-induced linear damping term [4]. Both the damping term, caused by the vibrations of the transverse components of the relative velocities between the pads and the disk, and the gyroscopic terms affect the stability of the system and they both depend on the macroscopic angular velocity of the disk [5]. Besides models with continua, models with wobbling disk can also capture these terms; therefore, some models have been developed in this

way to study the mechanism of brake squeal: minimal model with 2 DOFs [6], 2-DOF model with in-plane vibration of the pads [7], 6-DOF model [5] and 8-DOF model [8]. In those studies, a specialized commercial software called Autolev [9] was required to obtain the final form of the equations of motion, which is quite inconvenient for further generalization. It should also be noted that there is still room for improvement: to the authors' best knowledge, asymmetric friction coefficients have not been considered anywhere, and the existing models omit either some dampers or in-plane vibrations of the pads.

The purpose of this paper is to create a procedure to establish the equations of motions of models with wobbling disk that can be implemented by more popular computing software. For this to happen, a recently developed matrix form of Euler equations in rigid body dynamics is adopted. The effects of tangential springs and asymmetric friction coefficients on stability are also discussed.

2. EULER EQUATIONS OF A LOW-DOF BRAKE SYSTEM MODEL WITH WOBBLING DISK AND FRICTIONAL POINT CONTACTS

The brake disk is considered as a rigid circular disk fixed at O - a point on its axis of symmetry that is perpendicular to its surfaces (Fig. 1a) [10]. Supported by rotational springs k_t and rotational dampers d_t, it lies horizontally at equilibrium, and it is driven by a torque M_A. Each of the two pads is modeled as a massless element supported in normal direction by a linear spring (k_1 on the upper half, k_2 lower half) and a damper (d_1 on the upper half, d_2 lower half) and in tangential direction by another linear spring (k_{ip1} on the upper half, k_{ip2} lower half). The visco-elastic supports in normal direction are preloaded by forces N_0. The coefficients of kinetic friction at the upper and lower contact points are μ_{k1} and μ_{k2}, respectively. Compared with the model presented here, the model in [6] does not consider the tangential springs and the model in [7] does not have any dampers, and both of them are absolutely symmetrical about the disk.

The fixed frame system $Ox_0y_0z_0$ is chosen such that Oz_0 is perpendicular to the surfaces of the disk and both the contact points lie on the plane Oy_0z_0 when the disk is at equilibrium. The body-fixed frame $Ox_3y_3z_3$ coincides with $Ox_0y_0z_0$ when the disk is at equilibrium. The position of the disk can be determined by three Cardan angles q_1, q_2 and q_3 which are angles of rotation about x_0-, y_1- and z_2-axis respectively, where $Ox_1y_1z_1$ and $Ox_2y_2z_2$ are intermediate frames (Fig. 1b). Hence, the vector of generalized coordinates is

$$\mathbf{q} = \begin{bmatrix} q_1 & q_2 & q_3 \end{bmatrix}^T . \tag{1}$$

The direction cosine matrices of the frames are determined as

$$^0\mathbf{A}_1 = \mathbf{R}(x, q_1) , \tag{2}$$

$$^0\mathbf{A}_2 = \mathbf{R}(x, q_1)\mathbf{R}(y, q_2) , \tag{3}$$

$$\mathbf{A} = {}^0\mathbf{A}_3 = \mathbf{R}(x, q_1)\mathbf{R}(y, q_2)\mathbf{R}(z, q_3) , \tag{4}$$

where $\mathbf{R}(*,q)$ is the elementary rotation matrix around axis * by an angle q [11]. Each column of a direction cosine matrix is a unit vector in the corresponding frame, i.e.

$$^0\mathbf{A}_i = \left[\mathbf{x}_i^{(0)}, \mathbf{y}_i^{(0)}, \mathbf{z}_i^{(0)} \right] \quad (i = 1, 2, 3). \tag{5}$$

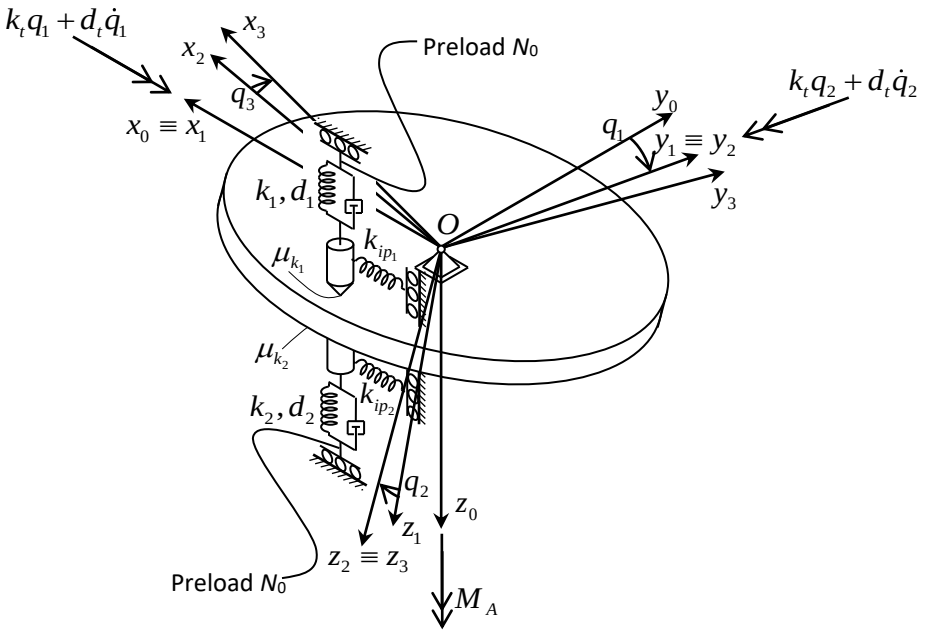

a) A low-DOF brake system model with wobbling disk and frictional point contacts [10]

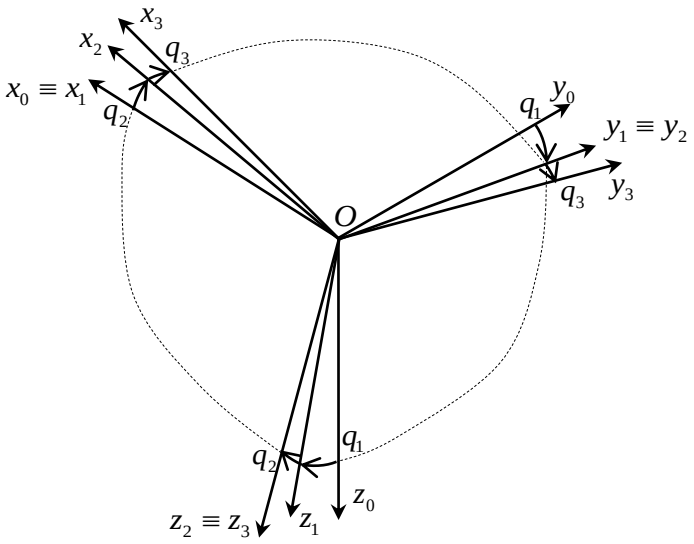

b) Coordinate systems

Figure 1. A low-DOF system model for brake squeal and its coordinate systems.

The total angular velocity of the disk can be written on the fixed frame or on the body-fixed frame

$$\boldsymbol{\omega}^{(0)} = \mathbf{J}_R^{(0)}(\mathbf{q})\dot{\mathbf{q}}\,, \tag{6}$$

$$\boldsymbol{\omega}^{(3)} = \mathbf{J}_R^{(3)}(\mathbf{q})\dot{\mathbf{q}} \tag{7}$$

where $\mathbf{J}_R^{(\cdot)}$ are rotational Jacobian matrices, which can be determined as

$$\mathbf{J}_R^{(0)}(\mathbf{q}) = \left[\mathbf{x}_1^{(0)}, \mathbf{y}_2^{(0)}, \mathbf{z}_3^{(0)}\right], \tag{8}$$

$$\mathbf{J}_R^{(3)}(\mathbf{q}) = \mathbf{A}^T \mathbf{J}_R^{(0)}(\mathbf{q}). \tag{9}$$

Rotational Hessian matrices are the partial derivatives of rotational Jacobian matrices with respect to the vector of generalized coordinates [12]. It is noted that the partial derivative of a matrix with respect to a vector is defined in [13, 14].

$$\mathbf{H}_R^{(0)}(\mathbf{q}) = \frac{\partial \mathbf{J}_R^{(0)}(\mathbf{q})}{\partial \mathbf{q}}, \tag{10}$$

$$\mathbf{H}_R^{(3)}(\mathbf{q}) = \frac{\partial \mathbf{J}_R^{(3)}(\mathbf{q})}{\partial \mathbf{q}}. \tag{11}$$

The positions of the contact points can be determined on the trajectories of the pads

$$\mathbf{p}_1^{(0)} = \mathbf{p}_{I_1}^{(0)} + \mathbf{z}_0^{(0)} h_1, \tag{12}$$

$$\mathbf{p}_2^{(0)} = \mathbf{p}_{I_2}^{(0)} + \mathbf{z}_0^{(0)} h_2 \tag{13}$$

with

$$\mathbf{p}_{I_1}^{(0)} = \begin{bmatrix} l_1 & -r & -h_{10} \end{bmatrix}^T, \tag{14}$$

$$\mathbf{p}_{I_2}^{(0)} = \begin{bmatrix} l_2 & -r & h_{20} \end{bmatrix}^T, \tag{15}$$

$$\begin{bmatrix} u_i & v_i & h_i \end{bmatrix}^T = \begin{bmatrix} \mathbf{A}\mathbf{x}_3^{(3)} & \mathbf{A}\mathbf{y}_3^{(3)} & -\mathbf{z}_0^{(0)} \end{bmatrix}^{-1} (\mathbf{p}_{I_i}^{(0)} - \mathbf{A}\mathbf{p}_{K_i}^{(3)}),\ i = 1,2, \tag{16}$$

$$\mathbf{p}_{K_1}^{(0)} = \begin{bmatrix} 0 & 0 & -h_{10} \end{bmatrix}^T, \tag{17}$$

$$\mathbf{p}_{K_2}^{(0)} = \begin{bmatrix} 0 & 0 & h_{20} \end{bmatrix}^T \tag{18}$$

in which h_{10} and h_{20} are respectively the distances from O to the upper and lower surfaces of the disk; h_1 and h_2 are respectively the z_0-direction displacements of the upper and lower pads from the disk equilibrium; l_1 and l_2 are respectively the deformed length of the upper and lower tangential springs, measured from the state of the "silent motion"; and r is the effective braking radius. Because the fixed frame and the body-fixed frame have the same origin, the position vectors of the contact points in the body-fixed frame can be simply determined as

$$\mathbf{p}_1^{(3)} = \mathbf{A}^T \mathbf{p}_1^{(0)}, \tag{19}$$

$$\mathbf{p}_2^{(3)} = \mathbf{A}^T \mathbf{p}_2^{(0)}. \tag{20}$$

The relative velocities of the contact points with respect to the disk are

$$\mathbf{v}_{r_1}^{(3)} = \frac{\mathrm{d}}{\mathrm{d}t}\mathbf{p}_1^{(3)} = \frac{\mathrm{d}}{\mathrm{d}t}(\mathbf{A}^T \mathbf{p}_1^{(0)}), \tag{21}$$

$$\mathbf{v}_{r_2}^{(3)} = \frac{\mathrm{d}}{\mathrm{d}t}\mathbf{p}_2^{(3)} = \frac{\mathrm{d}}{\mathrm{d}t}(\mathbf{A}^T \mathbf{p}_2^{(0)}), \tag{22}$$

and rewriting them in the fixed frame yields

$$\mathbf{v}_{r_1}^{(0)} = \mathbf{A}\frac{\mathrm{d}}{\mathrm{d}t}(\mathbf{A}^T\mathbf{p}_1^{(0)}), \tag{23}$$

$$\mathbf{v}_{r_2}^{(0)} = \mathbf{A}\frac{\mathrm{d}}{\mathrm{d}t}(\mathbf{A}^T\mathbf{p}_2^{(0)}). \tag{24}$$

Thus, the directions of the friction forces acting on the disk are defined as

$$\mathbf{t}_{p_1}^{(0)} = \frac{\mathbf{v}_{r_1}^{(0)}}{\left|\mathbf{v}_{r_1}^{(0)}\right|}, \tag{25}$$

$$\mathbf{t}_{p_2}^{(0)} = \frac{\mathbf{v}_{r_2}^{(0)}}{\left|\mathbf{v}_{r_2}^{(0)}\right|}. \tag{26}$$

Each contact force is divided into two components

$$\mathbf{f}_{p_1}^{(0)} = F_{n_1}\mathbf{z}_3^{(0)} + F_{t_1}\mathbf{t}_{p_1}^{(0)}, \tag{27}$$

$$\mathbf{f}_{p_2}^{(0)} = -F_{n_2}\mathbf{z}_3^{(0)} + F_{t_2}\mathbf{t}_{p_2}^{(0)}. \tag{28}$$

where

$$F_{n_1} = \frac{N_0 - h_1k_1 - \dot{h}_1d_1}{\mathbf{z}_0^{(0)T}\mathbf{z}_3^{(0)} + \mu_{k_1}\mathbf{z}_0^{(0)T}\mathbf{t}_{p_1}^{(0)}}, \tag{29}$$

$$F_{n_2} = \frac{N_0 + h_2k_2 + \dot{h}_2d_2}{\mathbf{z}_0^{(0)T}\mathbf{z}_3^{(0)} - \mu_{k_2}\mathbf{z}_0^{(0)T}\mathbf{t}_{p_2}^{(0)}}, \tag{30}$$

$$F_{t_1} = \mu_{k_1}F_{n_1}, \tag{31}$$

$$F_{t_2} = \mu_{k_2}F_{n_2}. \tag{32}$$

The value of l_1 and l_2 can be determined as

$$l_1 = \frac{-F_{n_1}\mathbf{x}_0^{(0)T}\mathbf{z}_3^{(0)} - F_{t_1}\mathbf{x}_0^{(0)T}\mathbf{t}_{p_1}^{(0)}}{k_{ip_1}} - \frac{\mu_{k_1}N_0}{k_{ip_1}}, \tag{33}$$

$$l_2 = \frac{F_{n_2}\mathbf{x}_0^{(0)T}\mathbf{z}_3^{(0)} - F_{t_2}\mathbf{x}_0^{(0)T}\mathbf{t}_{p_2}^{(0)}}{k_{ip_2}} - \frac{\mu_{k_2}N_0}{k_{ip_2}}. \tag{34}$$

The recently developed matrix form of Euler equations helps to write the equations of motion of the disk in a compact form [10, 15]

$$\mathbf{M}^{(0)}(\mathbf{q})\ddot{\mathbf{q}} + \mathbf{C}^{*(0)}(\mathbf{q})(\dot{\mathbf{q}}\otimes\dot{\mathbf{q}}) = \sum\mathbf{m}^{(0)} \tag{35}$$

in which

$$\mathbf{M}^{(0)}(\mathbf{q}) = \mathbf{A}\mathbf{I}^{(3)}\mathbf{J}_R^{(3)}(\mathbf{q}), \tag{36}$$

$$\mathbf{C}^{*(0)}(\mathbf{q}) = \mathbf{A}\mathbf{I}^{(3)}\mathbf{H}_R^{(3)}(\mathbf{q}) + \mathbf{A}\tilde{\mathbf{J}}_R^{(3)}((\mathbf{I}^{(3)}\mathbf{J}_R^{(3)}(\mathbf{q}))\otimes\mathbf{E}_3)), \tag{37}$$

$$\sum\mathbf{m}^{(0)} = -\mathbf{x}_0^{(0)}(k_tq_1 + d_t\dot{q}_1) - \mathbf{y}_1^{(0)}(k_tq_2 + d_t\dot{q}_2) + \mathbf{z}_0^{(0)}M_A + \tilde{\mathbf{p}}_1^{(0)}\mathbf{f}_{p_1}^{(0)} + \tilde{\mathbf{p}}_2^{(0)}\mathbf{f}_{p_2}^{(0)} \tag{38}$$

where $\mathbf{I}^{(3)} = \mathrm{diag}([\Theta,\Theta,\Phi])$ is a matrix of constant representing the inertia tensor in body-fixed frame, $\mathbf{E}_k$ is the k-by-k identity matrix, $\otimes$ denotes the Kronecker product [16], and ~ operator is defined in [10, 12].

The matrix determined by (36) is not generally symmetric. Considering (9), one can simply multiply $\mathbf{J}_R^{(0)T}(\mathbf{q})$ by the left of (36) to obtain a symmetric matrix

$$\mathbf{J}_R^{(0)T}(\mathbf{q})\mathbf{M}^{(0)}(\mathbf{q}) = \mathbf{J}_R^{(0)T}(\mathbf{q})\mathbf{A}\mathbf{I}^{(3)}\mathbf{J}_R^{(3)}(\mathbf{q}) = \mathbf{J}_R^{(3)T}(\mathbf{q})\mathbf{I}^{(3)}\mathbf{J}_R^{(3)}(\mathbf{q}) = (\mathbf{J}_R^{(3)T}(\mathbf{q})\mathbf{I}^{(3)}\mathbf{J}_R^{(3)}(\mathbf{q}))^T . \tag{39}$$

It implies that the inertia matrix in (35) can be symmetrized in the same way. However, (35) is the better choice in this paper due to the fact that the driving torque M_A only appears in the third equation of (38) and, therefore, does not appear in the first two equations of (35). This property allows the reduction of the number of degrees of freedom from three to two in the next chapter without considering M_A.

3. NON-HOLONOMIC CONSTRAINT AND LINEARIZATION

The disk is considered to be subjected to a non-holonomic constraint that the z_0-component of the angular velocity of the disk has a constant value Ω_d as follows

$$\mathbf{z}_0^{(0)T}\boldsymbol{\omega}^{(0)} = \dot{q}_2 \sin q_1 + \dot{q}_3 \cos q_1 \cos q_2 = \Omega_d . \tag{40}$$

This constraint is one of the reasons that Autolev is required in the previous studies. Using the Kronecker product, this problem can be overcome with ease. Equation (40) can be rewritten as

$$\dot{\mathbf{q}} = \mathbf{s}(\mathbf{q}_m) + \mathbf{S}(\mathbf{q}_m)\dot{\mathbf{q}}_m . \tag{41}$$

where

$$\mathbf{q}_m = \begin{bmatrix} q_1 & q_2 \end{bmatrix}^T ,\ \mathbf{s}(\mathbf{q}_m) = \begin{bmatrix} 0 & 0 & \dfrac{\Omega_d}{\cos q_1 \cos q_2} \end{bmatrix}^T ,\ \mathbf{S}(\mathbf{q}_m) = \begin{bmatrix} 1 & 0 & 0 \\ 0 & 1 & \dfrac{-\sin q_1}{\cos q_1 \cos q_2} \end{bmatrix}^T . \tag{42}$$

Multiplying the left of both sides of (35) by

$$\mathbf{G} = \begin{bmatrix} 1 & 0 & 0 \\ 0 & 1 & 0 \end{bmatrix} \tag{43}$$

and using (42), one obtains

$$\boldsymbol{\psi} = \mathbf{M}_m\ddot{\mathbf{q}}_m + \mathbf{C}_m^*(\dot{\mathbf{q}}_m \otimes \dot{\mathbf{q}}_m) + \mathbf{D}_m\dot{\mathbf{q}}_m + \mathbf{K}_m\mathbf{q}_m - \mathbf{f}_m = 0 \tag{44}$$

where

$$\mathbf{M}_m(\mathbf{q}_m) = \mathbf{G}\mathbf{M}^{(0)}\mathbf{S} ,\ \mathbf{C}_m^*(\mathbf{q}_m) = \mathbf{G}\mathbf{M}^{(0)}\frac{\partial \mathbf{S}}{\partial \mathbf{q}_m} + \mathbf{G}\mathbf{C}^{*(0)}(\mathbf{S} \otimes \mathbf{S}) ,$$

$$\mathbf{D}_m(\mathbf{q}_m) = \mathbf{G}\mathbf{M}^{(0)}\frac{\partial \mathbf{s}}{\partial \mathbf{q}_m} + \mathbf{G}\mathbf{C}^{*(0)}(\mathbf{s} \otimes \mathbf{S} + \mathbf{S} \otimes \mathbf{s}) + \begin{bmatrix} d_t & 0 \\ 0 & d_t \cos q_1 \end{bmatrix},$$

$$\mathbf{K}_m(\mathbf{q}_m) = \begin{bmatrix} k_t & 0 \\ 0 & k_t \cos q_1 \end{bmatrix},\ \mathbf{f}_m(\mathbf{q}_m) = \mathbf{G}\tilde{\mathbf{p}}_1^{(0)}\mathbf{f}_{p_1}^{(0)} + \mathbf{G}\tilde{\mathbf{p}}_2^{(0)}\mathbf{f}_{p_2}^{(0)} . \tag{45}$$

To perform linearization, the silent motion

$$\mathbf{q}_m(t) = \mathbf{q}_{m_0} = \mathbf{const} \tag{46}$$

must be found first by substituting $\dot{\mathbf{q}}_m(t) = \ddot{\mathbf{q}}_m(t) = \mathbf{0}$; $\dot{l}_1 = \dot{l}_2 = 0$ into (44). Then, linearizing (44) around the silent motion yields

$$\bar{\mathbf{M}}_m \delta\ddot{\mathbf{q}}_m + \bar{\mathbf{D}}_m \delta\dot{\mathbf{q}}_m + \bar{\mathbf{K}}_m \delta\mathbf{q}_m = \mathbf{0} \tag{47}$$

where

$$\bar{\mathbf{M}}_m = \left.\frac{\partial \boldsymbol{\psi}_m}{\partial \ddot{\mathbf{q}}_m}\right|_{\mathbf{q}_{m_0}}, \ \bar{\mathbf{D}}_m = \left.\frac{\partial \boldsymbol{\psi}_m}{\partial \dot{\mathbf{q}}_m}\right|_{\mathbf{q}_{m_0}}, \ \bar{\mathbf{K}}_m = \left.\frac{\partial \boldsymbol{\psi}_m}{\partial \mathbf{q}_m}\right|_{\mathbf{q}_{m_0}}. \tag{48}$$

3. DISCUSSION

3.1. Effects of tangential springs on the stability map

The appearance of friction forces whose directions vary in 3D space increases the complexity of writing the equations of motion. Moreover, analytically solving the silent motion is complicated, unless it is the trivial solution. Hence, in a general case, the symbolic forms of the matrices in (47) are cumbersome and hard to write down manually. The trivial solution is valid if and only if the following condition holds

$$\boldsymbol{\psi}\big|_{\mathbf{q}=0,\dot{\mathbf{q}}=\mathbf{0},\mathbf{q}=\mathbf{0},\dot{l}_1=\dot{l}_2=0} = \begin{bmatrix} 0 \\ -N_0(\mu_{k_1} h_{10} - \mu_{k_2} h_{20}) \end{bmatrix} = \mathbf{0}. \tag{49}$$

A case that is normally considered is

$$h_{10} = h_{20} = h/2, \ \mu_{k_1} = \mu_{k_2} = \mu_k. \tag{50}$$

The matrices of the linearized equations are

$$\bar{\mathbf{M}}_m = \begin{bmatrix} \Theta & 0 \\ 0 & \Theta \end{bmatrix}, \tag{51}$$

$$\bar{\mathbf{D}}_m = \begin{bmatrix} d_t + (d_1+d_2)r^2 + \dfrac{\mu_k^2 N_0 h}{2}\left(\dfrac{d_1}{k_{ip_1}} + \dfrac{d_2}{k_{ip_2}}\right) + \dfrac{\mu_k N_0 h^2}{2\Omega_d r} & \Phi\Omega_d \\ \mu_k N_0 r\left(\dfrac{d_1}{k_{ip_1}} + \dfrac{d_2}{k_{ip_2}}\right) - (d_1+d_2)\dfrac{\mu_k h r}{2} - \Phi\Omega_d & d_t \end{bmatrix}, \tag{52}$$

$$\bar{\mathbf{K}}_m = \begin{bmatrix} k_t + N_0 h + (k_1+k_2)r^2 + \dfrac{\mu_k^2 N_0 h}{2}\left(\dfrac{k_1}{k_{ip_1}} + \dfrac{k_2}{k_{ip_2}}\right) & \dfrac{\mu_k N_0 h}{2r}\left(h - (1+\mu_k^2)\left(\dfrac{N_0}{k_{ip_1}} + \dfrac{N_0}{k_{ip_2}}\right)\right) \\ -\mu_k r\left(2N_0 - \dfrac{N_0 k_1}{k_{ip_1}} - \dfrac{N_0 k_2}{k_{ip_2}} + \dfrac{k_1 h}{2} + \dfrac{k_2 h}{2}\right) & k_t + (1+\mu_k^2)N_0\left(h - \dfrac{N_0}{k_{ip_1}} - \dfrac{N_0}{k_{ip_2}}\right) \end{bmatrix}. \tag{53}$$

Some intermediate results for this case can be found in [10]. There are also extended models with complex friction formulations or more DOFs added to the pads' mounting mechanism. The use of the Kronecker product not only makes it much easier to write down and simplify necessary formulations such as the Euler equations and the linear non-holonomic constraint but also reduces 5% of CPU time to produce the symbolic nonlinear equations compared to the case without the Kronecker product. The matrices (51)-(53) agree with [6]

$$\bar{\mathbf{M}}_m = \begin{bmatrix} \Theta & 0 \\ 0 & \Theta \end{bmatrix}, \ \bar{\mathbf{D}}_m = \begin{bmatrix} d_t + 2dr^2 + \dfrac{\mu_k N_0 h^2}{2\Omega_d r} & \Phi\Omega_d \\ -\Phi\Omega_d - \mu_k d h r & d_t \end{bmatrix}, \ \bar{\mathbf{K}}_m = \begin{bmatrix} k_t + N_0 h + 2kr^2 & \dfrac{\mu_k N_0 h^2}{2r} \\ -\mu_k r(2N_0 + kh) & k_t + (1+\mu_k^2)N_0 h \end{bmatrix} \tag{54}$$

by considering the case where the visco-elastic supports of the pads are symmetric and the pads have no in-plane movement, i.e. the in-plane stiffnesses are infinity

$$d_1 = d_2 = d\ ,\ k_1 = k_2 = k\ ,\ \frac{1}{k_{ip1}} = \frac{1}{k_{ip2}} = 0\ . \tag{55}$$

It is interesting to point out that, in contrast to the normal stiffnesses, the tangential stiffnesses k_{ip1} and k_{ip2} appear in the damping matrix in equation (52). It is not unreasonable due to the fact that the considered model is complicated in terms of spatial motion and frictional contacts, so **D** may contain terms resulted from other interactions, not just damping coefficients and gyroscopic terms. To perform stability analysis, the parameters are chosen from the literature [6], [10] as follows:

$h = 0.02$ m; $r = 0.13$ m; $\Theta = 0.16$ kgm^2; $\Phi = 2\Theta$; $k_t = 1.88\times10^7$ Nm; $d_t = 0.1$ Nms;

$k = k_1 = k_2 = 6\times10^6$ N/m; $d = d_1 = d_2 = 5$ Ns/m;

$k_{ip} = k_{ip_1} = k_{ip_2}$; $\Omega = 8\times 2\pi$ rad/s; $N_0 = \dfrac{1800}{\mu_k}$ N.

A stability map with varying k_{ip} and μ_k is shown in Fig. 2. It can be seen that while k_{ip} decreases along the dashed line in Fig. 2, there are two points where the system changes its stability. At point A it moves from the unstable region to the stable one and at point B it moves back to theformer. This means that for the given parameters, decreasing k_{ip} may either stabilize or destabilize the trivial solution of the system. The stabilizing effect may be explained by the fact that when both k_{ip1} and k_{ip2} decrease, the first element of the first row of the damping matrix in equation (52) increases, adding more damping to the system. However, the tangential stiffnesses also appear in the first element of the second row of the damping matrix in equation (52) as well as all four elements of the stiffness matrix in equation (53), which may be the reason for the destabilizing effect.

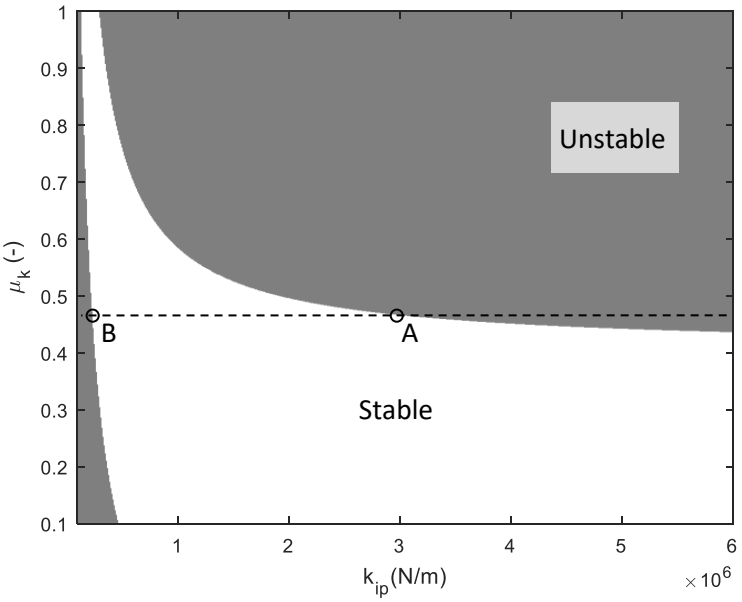

Figure 2. Stability diagram with varied tangential stiffness and kinetic coefficients of friction.

3.2. Effects of asymmetric friction coefficients on the stability map

It is more realistic to choose different coefficients of friction at upper and lower contact points. Although the pads of the same type are usually used, they are not perfectly identical and may produce different friction coefficients when in contact with the disk, especially under the effects of conditions such as temperature and wear.

Considering the case where the supports of the pads are symmetrical

$$d_1 = d_2 = d\ ,\ k_1 = k_2 = k\ ,\ k_{ip1} = k_{ip2} = k_{ip} \tag{56}$$

and (49) is satisfied, but the coefficients of kinetic friction of the upper and lower contact may be different from each other, i.e.

$$\mu_{k_1} h_{10} = \mu_{k_2} h_{20} = \frac{h\mu_{k_1}\mu_{k_2}}{\mu_{k_1} + \mu_{k_2}} \tag{57}$$

where

$$h = h_{10} + h_{20} \tag{58}$$

is the thickness of the disk.

The matrices of the linearized equations read

$$\bar{\mathbf{M}}_m = \begin{bmatrix} \Theta & 0 \\ 0 & \Theta \end{bmatrix}, \tag{59}$$

$$\bar{\mathbf{D}}_m = \begin{bmatrix} d_t + 2dr^2 + \dfrac{N_0 dh\mu_{k_1}\mu_{k_2}}{k_{ip}} + \dfrac{N_0}{\Omega_d r}\dfrac{h^2\mu_{k_1}\mu_{k_2}}{\mu_{k_1}+\mu_{k_2}} & \Phi\Omega_d \\ \dfrac{N_0 dr}{k_{ip}}(\mu_{k_1}+\mu_{k_2}) - \dfrac{2h\mu_{k_1}\mu_{k_2}dr}{\mu_{k_1}+\mu_{k_2}} - \Phi\Omega_d & d_t \end{bmatrix}, \tag{60}$$

$$\bar{\mathbf{K}}_m = \begin{bmatrix} k_t + N_0 h + 2kr^2 + \dfrac{N_0 k}{k_{ip}} h\mu_{k_1}\mu_{k_2} & \dfrac{N_0 h^2 \mu_{k_1}\mu_{k_2}}{r(\mu_{k_1}+\mu_{k_2})} - \dfrac{N_0^2 h\mu_{k_1}\mu_{k_2}}{rk_{ip}(\mu_{k_1}+\mu_{k_2})}(2+\mu_{k_1}^2+\mu_{k_2}^2) \\ -rN_0(\mu_{k_1}+\mu_{k_2})\left(1-\dfrac{k}{k_{ip}}\right) - \dfrac{2rkh\mu_{k_1}\mu_{k_2}}{\mu_{k_1}+\mu_{k_2}} & k_t + N_0 h(1+\mu_{k_1}\mu_{k_2}) - \dfrac{N_0^2}{k_{ip}}(2+\mu_{k_1}^2+\mu_{k_2}^2) \end{bmatrix}. \tag{61}$$

The following parameters are used:

$h = 0.02$ m; $r = 0.13$ m; $\Phi = 0.32$ kg/m^2; $k_t = 1.88\times10^7$ Nm; $d_t = 0.1$ Nms;

$k = 6\times10^6$ N/m; $d = 5$ Ns/m; $N_0 = 3000$ N.

The coefficients are varied but their sum is kept as high as 1

$$\mu_{k_1} + \mu_{k_2} = 1. \tag{62}$$

The distances h_{10} and h_{20} are computed from the friction coefficients satisfying (57). Assuming the brake disk is a thin homogeneous disk with a radius of 0.15 m, one can determine the moment of inertia of the disk about Ox_3 or Oy_3 as follows

$$\Theta = \frac{\Phi}{2} + \frac{\Phi}{0.045}\left(h_{10} - h_{20}\right)^2. \tag{63}$$

Fig. 3 shows the dependence of critical speed Ω_{crit} – the threshold that when Ω exceeds, the trivial solution of the system becomes unstable – on $\mu_{k_1} - \mu_{k_2}$. The graphs are U-shaped, meaning that increasing the difference between the friction coefficients may stabilize the trivial solution of the system.

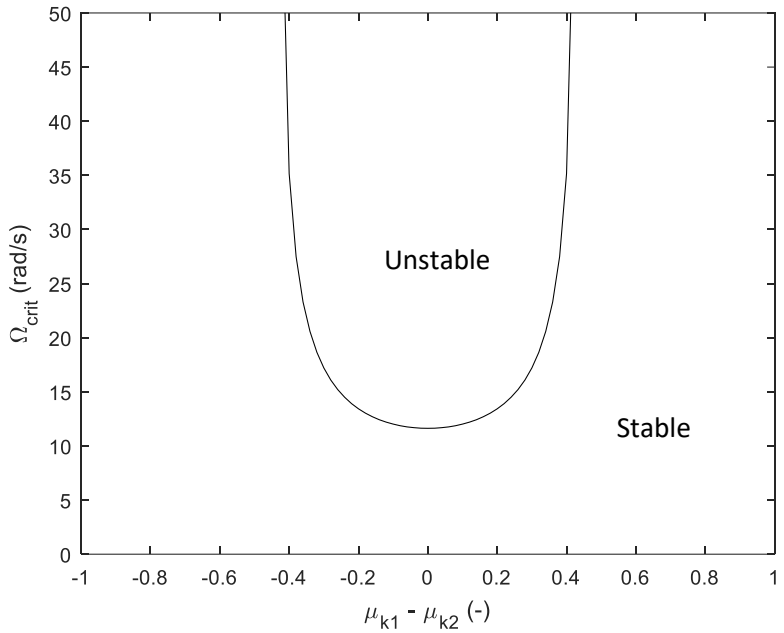

Figure 3. Critical speed for asymmetric coefficients of kinetic friction.

4. CONCLUSIONS AND OUTLOOK

A general asymmetric low-DOF model with wobbling disk for brake squeal has been presented. Using the recently developed matrix form of Euler equations, a procedure for establishing the equations of motion of the model has been constructed. The linear non-holonomic constraint has been processed with the help of the Kronecker product. Computer aid is needed because of the complexity of the kinematics of the contact points and linearization. However, unlike previous studies, no specialized software is required, a popular technical computing software is enough.

The stability analysis shows that increasing the difference between the coefficients of kinetic friction while keeping their sum constant may have stabilizing effect. Decreasing the stiffnesses of tangential springs can either stabilize or destabilize the trivial solution of the system.

More complicated friction models will be embedded into the model and the procedure will be used to analyze the dynamics of the model to study the origin and characteristics of brake squeal and contribute to the development of a silent brake.

Acknowledgements. This research is funded by the Hanoi University of Science and Technology (HUST) under project number T2018-PC-213.

CRediT authorship contribution statement: Nguyen Thai Minh Tuan: Methodology, Software, Formal analysis, Writing. Nils Gräbner: Conceptualization, Validation, Resources.

Declaration of competing interest: The authors declare that they have no known competing financial interests or personal relationships that could have appeared to influence the work reported in this paper.

REFERENCES

1. Shin K., Brennan M. J., Oh J. E., Harris C. J. - Analysis of disc brake noise using a two-degree-of-freedom model, Journal of Sound and Vibration **254** (5) (2002) 837-848.
2. Hoffmann N., Fischer M., Allgaier R., Gaul L. - A minimal model for studying properties of the mode-coupling type instability in friction induced oscillations, Mechanics Research Communications **29** (4) (2002) 197-205.
3. Popp K., Rudolph M., Kröger M., Lindner M. - Mechanisms to generate and to avoid friction induced vibrations, VDI-Bericht **1736** (2002) 1-15.
4. Hochlenert D., Spelsberg-Korspeter G., Hagedorn P. - Friction induced vibrations in moving continua and their application to brake squeal, Journal of Applied Mechanics **74** (3) (2007) 542-549.
5. Gräbner N. - Analyse und Verbesserung der Simulationsmethode des Bremsenquietschens (in German) (Doctoral dissertation). Technische Universität Berlin, Germany, 2016.
6. von Wagner U., Hochlenert D., Hagedorn P. - Minimal models for disk brake squeal, Journal of Sound and Vibration **302** (3) (2007) 527-539.
7. von Wagner U., Schlagner S. - Beurteilung des Geräuschverhaltens von Scheibenbremsen mit Hilfe von piezokeramischen Aktoren und Sensoren (in German), VDI-Berichte **1982** (2007) 151-165.
8. Koch S., Gräbner N., Gödecker H., von Wagner U. - Nonlinear Multiple Body Models for Brake Squeal, PAMM **17** (1) (2017) 33-36.
9. Kane T. R., Levinson D. A. - Dynamics: Theory and Applications, McGraw-Hill, New York, 1985.
10. Nguyen Thai Minh Tuan - Effect of vibrations on friction in the context of brake squeal (Doctoral dissertation), Technische Universität Berlin, Germany, 2019.
11. Schiehlen W., Eberhard P. - Applied Dynamics, Vol. 57, Springer, Berlin, 2014.
12. Nguyen Thai Minh Tuan, Pham Thanh Chung, Do Dang Khoa, Phan Dang Phong - Kinematic and dynamic analysis of multibody systems using the Kronecker product, Vietnam Journal of Science and Technology **57** (1) (2019) 112-127.
13. Nguyen Van Khang - Consistent definition of partial derivatives of matrix functions in dynamics of mechanical systems, Mechanism and Machine Theory **45** (2010) 981-988.
14. Nguyen Van Khang - Partial derivative of matrix functions with respect to a vector variable, Vietnam Journal of Mechanics **30** (4) (2008) 269-279.
15. Nguyen Thai Minh Tuan - The matrix form of Newton-Euler equations for spatial bodies with Kronecker product (in Vietnamese), In Proceedings of the 1st National Conference on Dynamics and Control, Da Nang, Vietnam, 2019, 196-200.
16. Brewer, J. - Kronecker products and matrix calculus in system theory, IEEE Transactions on circuits and systems **25** (9) (1978) 772-781.